

# SEACOW: Synopsis Embedded Array Compression using Wavelet Transform

Minsoo Kim  
Korea University  
Seoul, Republic of Korea  
msdb@korea.ac.kr

Hyubjin Lee  
Korea University  
Seoul, Republic of Korea  
hyubjinlee@korea.ac.kr

Yon Dohn Chung\*  
Korea University  
Seoul, Republic of Korea  
ydchung@korea.ac.kr

## ABSTRACT

Recently, multidimensional data is produced in various domains; because a large volume of this data is often used in complex analytical tasks, it must be stored compactly and able to respond quickly to queries. Existing compression schemes well reduce the data storage; however, they might increase overall computational costs while performing queries. Effectively querying compressed data requires a compression scheme carefully designed for the tasks.

This study presents a novel compression scheme, SEACOW, for storing and querying multidimensional array data. The scheme is based on wavelet transform and utilizes a hierarchical relationship between sub-arrays in the transformed data to compress the array. A result of the compression embeds a synopsis, improving query processing performance while acting as an index. To perform experiments, we implemented an array database, SEACOW storage, and evaluated query processing performance on real data sets. Our experiments show that 1) SEACOW provides a high compression ratio comparable to existing compression schemes and 2) the synopsis improves analytical query processing performance.

## 1 INTRODUCTION

Multidimensional data is used in various domains, including sensor data from earth sciences, medical images from life science, and observation data from astronomy telescopes. Commercial applications, such as financial, statistical, and stock data, also produce multidimensional data. These types of data tend toward massive volumes continuous growth. Because they require a large storage space, they are commonly compressed in storage systems.

Commonly involved in exploration and analysis tasks, using these datasets can incur huge computing costs [3]. Exploration queries on the multidimensional array are categorized by predicate type: dimension-based or value-based exploration. A dimension-based exploration query specifies a region of interest on its dimensions, defined by the ranges of consecutive values for each dimension in the multidimensional data. This type of query is frequently used to set the boundaries for following analytical tasks and exclude the rest of the data. For example, zooming in on a hurricane to better visualize a section on a weather radar map is a dimension-based exploration. A value-based exploration query filter out specific elements, leaving only the desired information. It often utilizes indices to quickly recognize the location of the required element. For example, a value-based exploration task that selects white pixels in a color mosaic map of Mars in order to measure the volume of water ice on the planet's surface.

Unsurprisingly, array databases [1, 12, 21] are well designed to support these types of workflows with multidimensional data. In an

array database, data are represented as a multidimensional indexed array, which enables rapid access to elements at a specific position. Subsequently, it supports the efficient process of dimension-based queries. They also offer several compression options as well as rich functions for analyzing the multidimensional data. For example, array databases [4, 12] embed array compression options, such as Lempel-Ziv [22], run-length encoding, null-suppression, and gzip, to handle massive amounts of data with fewer storage requirements. These well-known compression schemes are general purpose and store the array as highly compressed binary data. However, they might cause heavy computational cost to restore the compressed data to the plain array at the beginning of query processing. In addition, when a complex analysis task is accompanied by a decoding process, the overall cost increases more. Other than compression, none of the options offer any other features for query processing. Accordingly, existing data compression schemes supported by array databases have trade-offs.

On the other hand, many data processing domains—including text, image, and video processing—use their data-specific compression schemes. Each schemes was designed only for its individual data type, taking into account the characteristics of target data. For example, some image compression schemes support spatial random access, which allows the quick reading of any part of an image. However, some video compression schemes utilize the spatial temporal correlation of each pixel on the nature of the video data during the data compression process. They meet the requirements of an environment in which the data is used. Accordingly, the compression schemes used in databases require this approach as well.

In this paper, we propose a novel compression scheme, Synopsis Embedded Array Compression using Wavelet Transform (SEACOW), that meets the requirements of array databases. We designed our compression scheme with the following requirements: (1) It should provide a high compression ratio for multidimensional array data, and (2) It should provide features that facilitate query processing. The second requirement is essential in the database and differs from the existing methods. In particular, we focus on providing useful features for exploration queries with highly compressed arrays.

The contributions of this paper are as follows:

- (1) We propose a numerical array compression method, SEACOW, which supports efficient exploration query processing in a compressed array
- (2) We present algorithms to perform queries on a compressed array using SEACOW.
- (3) We implement a storage manager for a large-scale multidimensional array and perform experiments on the storage.

\*Corresponding author.

- (4) We evaluate the compression and query performance of our compression method, compared with those of existing methods.

The remainder of this paper is organized as follows. We describe the background and related work in Section 2. We present SEACOW in Section 3 and the query processing algorithm on a compressed array using SEACOW in Section 4. In Section 5, we present a performance comparison of SEACOW with other existing methods. Finally, we draw conclusions and discuss future work in Section 6.

## 2 BACKGROUND & RELATED WORK

### 2.1 Array data model

The array data model is composed of dimensions, cells, and attributes. The dimensions define a multidimensional space to represent the array data, and each dimension has consecutive integers with a range limitation. The  $n$ -dimensional array has a set of  $m$  dimensions  $\mathbb{D} = d_0, d_1, \dots, d_{m-1}$ . On each combination of dimension values, there is an array cell. Accordingly, an array cell has a particular location in a multidimensional space. It holds the fixed number of attributes, and its unique name identifies each attribute. For simplicity, in the rest of this paper, we assume that the array contains only one attribute.

In general, as multidimensional arrays are massive, they are partitioned into sub-arrays. The sub-arrays can overlap at their boundaries; however, we consider only non-overlapped sub-arrays in this study. There are several partitioning techniques, depending on the levels it takes and whether the sub-arrays are regular or not [17]. This paper uses chunking to refer to the array partitioning strategy and a chunk to refer to the partitioned sub-arrays. Considering the storage efficiency, we assumed non-overlapped chunks.

### 2.2 Wavelet transform

Wavelet transform, also known as wavelet decomposition, is a mathematical tool, which is widely used in signal processing. It decomposes the source data in different scales of wavelet functions. This method successively applies a low-pass and high-pass filter, followed by down-sampling by a factor of two. After transformation, the elements of the data are decomposed into approximation coefficients and detail coefficients at different resolutions. In this process, the overall size of the data remains the same.

Here, we provide an example of a one-dimensional discrete wavelet transform(DWT). We use Haar wavelet, which is the shortest well known wavelet. In the Haar wavelet, approximate coefficients can be computed by averaging the non-overlapped pairwise of the elements and detail coefficients are the differences of the approximate coefficients.

$$\psi(t) = \frac{1}{2} \begin{cases} 1, & \text{for } 0 \leq t < 1/2 \\ -1, & \text{for } 1/2 \leq t < 1 \\ 0, & \text{otherwise} \end{cases}$$

Suppose there is a one-dimensional array  $A = [71, 67, 60, 62, 60, 60, 67, 73]$ . In Haar wavelet, the 8 entries in the array  $A$  can be grouped and make four pairs  $A' = [[71, 67], [60, 62], [60, 60], [67, 73]]$ . Applying Haar wavelet to the first pair  $[71, 67]$ , the approximate

coefficient is 69 and the detail coefficient is 2 since  $(71 + 67)/2 = 69$  and  $71 - 69 = 2$ . Accordingly, the rest of pairs are calculated. At a result of the first level of wavelet transformation, a set of approximate coefficients are  $[69, 61, 60, 70]$  and a set of detail coefficients are  $[2, -1, 0, -3]$ . The second transform is only adapted in the approximate coefficients of the first level transform. Repeating the process in the first level, then, the result of the second transform is  $[65, 65]$  for approximate coefficients, and  $[4, -5]$  for the detail coefficients. As the approximate part still has two values, there could be one more transform. The third level of wavelet transformation produces  $[65]$  for the approximate coefficient, and  $[0]$  for the detail coefficient. Then,  $A$  is finally converted into  $W_A = [65, 0, 4, -5, 2, -1, 0, -3]$ . Each entry in  $W_A$  is called a wavelet coefficient. In the result, the final approximate coefficient 35 is an average of all entries in  $A$ .

**Table 1: Example of Haar wavelet transform.**

Resolution	Approximate Coefficients	Detail Coefficients
3	[71, 67, 60, 62, 60, 60, 67, 73]	–
2	[69, 61, 60, 70]	[2, -1, 0, -3]
1	[65, 65]	[4, -5]
0	[65]	[0]

The one-dimensional DWT can be extended to a multidimensional array. For example, in a two-dimensional array, the one-dimensional DWT is applied horizontally first to the rows of the array, and then, the transform is applied vertically to the columns. The two-dimensional array is decomposed into four sets of wavelet coefficients. This is the first level of a two-dimensional DWT.

Data compression is one of a well-known application of wavelet transform. In particular, the recent image compression standard JPEG 2000 [11] is based on wavelet transform. It provides a high compression ratio and many useful features, such as rich scalability, random spatial access, error resilience, and limited memory use.

### 2.3 Related work

**Data compression.** Although long studied in various domains, data compression is particularly important for database systems. Previous studies [7, 23] showed that data compression both improves query performance and reduces the storage requirements. Accordingly, existing databases provide numerous compression schemes in their storage systems. For simple compression, fixed-length coding techniques, such as bit-packing, encode elements in a fixed-length bit stream. However, the source data could have outliers that require larger fixed bits than the other elements and degrade the compression performance. Instead, PFOR, PFOR-DELTA, and PDICTION were introduced [26]. They exceptionally treat outliers and use more compact fixed bits for the others. Meanwhile, Lempel-Ziv [22, 25] and Huffman coding [8] are well-known compression schemes that use variable-length coding. They convert the fixed size of a symbol to a variable size of code words. Both of these general purpose fixed-length and variable-length coding algorithms can be applied to any data.

In array databases, they provide several compression options for storing and processing arrays. SciDB [1, 4] uses run-length encoding with null-suppression. TileDB [12] has conventional file

compression schemes, such as lz4, gzip, and bzip2. COMPASS [24], a specially designed array compression scheme, reorganizes array cells into a value-indexed representation. It is a bin-based algorithm that groups elements of similar value into the same bin. Value-based exploration can benefit from this representation. However, it is inadequate for queries with spatial access, such as dimension-based exploration and grid aggregation.

On the other hand, many compression schemes have been studied for multimedia data compression. The JPEG [20], a widely used image compression standard, is based on the Fourier transform. EZW [16] was newly designed for an image compression scheme based on the wavelet transform. Then, SPIHT [14] and EBCOT [18] improved the compression performance. Although designed for image data, these schemes often extend to compress array or numerical data. For example, image data can be treated as a two-dimensional array, and their compression schemes can also be extended to the array compression scheme. In [5, 19], image compression schemes compressed floating-point number data. Our work is also based on the wavelet transform.

**Synopsis.** Synopsis is a small summary of data, briefly describing the data. It is frequently used to improve query processing performance. Searchlight [10] utilizes multiple synopses with constraint programming. Searchlight first obtains the approximate answer from the synopses and performs a search query over large multidimensional data. Although various types of synopses can be used according to query type, the synopses occupy additional memory and storage space. Moreover, there is no compression option for the synopses.

Furthermore, researchers often use the wavelet synopsis for approximate query processing. Wavelet synopsis is a type of summary data produced during the wavelet transform. Chakrabarti et al. [2] and Garaofalakis et al. [6] provided general-purpose approximate query processing algorithms with wavelet synopses. Sacharidis et al. [13] proposed a compression scheme for wavelet synopses. However, they target only approximate query processing and focus on minimizing the error of the approximation, rather than exact query processing. Jahangiri et al. [9] used wavelet synopsis to range-group-by queries. In this study, they support both approximate and exact query processing algorithms. However, it is specialized only for dimension-based queries. ProDA [15] is an OLAP system that employs wavelets to manage massive data and support various types of queries.

### 3 SEACOW: THE PROPOSED METHOD

#### 3.1 Overview

In this section, we illustrate our array compression scheme, namely SEACOW. It compresses a multidimensional array with high compression ratio, while providing efficient exploration query performance. When compressed through SEACOW, compressed array consists of two parts: a synopsis and a body. The synopsis is a set of data structures that helps to enhance the compression ratio and is utilized as an index in query processing. It includes two data structures: Wavelet synopsis and HMMT. The synopsis is embedded in the compressed bit-stream of the array. Specifically, the synopsis part is located in front of the bit-stream and can be retrieved independently of the body. The second component, the body, contains

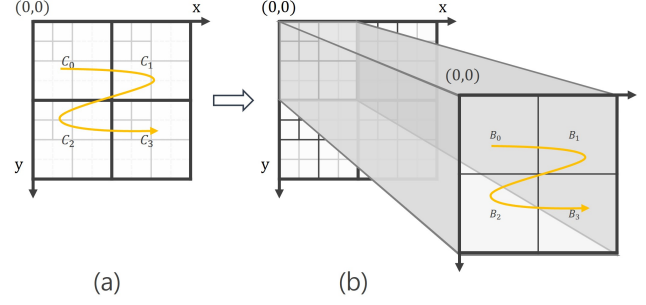


Figure 1: Example of a two-level chunking.

a set of real elements in the array. As the body contains all the detailed information to reconstruct the array, the compressed array can be reconstructed without any information loss.

#### 3.2 Array Chunking

An array in SEACOW is vertically partitioned by attributes, which is similar to columnar storage of relational databases. Then, an array of a single attribute is chunked into several small sub-arrays. In this division, SEACOW adapts two-level regular chunking, also known as regular-regular chunking [17]. The two-level regular chunking partitions an array into fixed-size chunks and divides the chunks once again into the fixed-size blocks. In the chunking strategy, the chunk, the larger one, is the unit of I/O, and the block, the smaller one, is the unit of query processing. Accordingly, each chunk is compressed individually and written on the disk, and vice versa. Note that, with some specific compression methods that support partial decoding, only a part of the array can be effectively restored into a plain sub-array. In this case, it is not necessary to decompress all the blocks in the chunk retrieved from the disk, but only some blocks can be decompressed.

Figure 1 shows an example of a two-level chunking with a two-dimensional  $8 \times 8$  array. The original array in Figure 1(a) splits into four  $4 \times 4$  chunks, such as  $C_0$ ,  $C_1$ ,  $C_2$ , and  $C_3$ . Then, the chunks are further divided into four  $2 \times 2$  blocks, such as  $B_0$ ,  $B_1$ ,  $B_2$ , and  $B_3$  in Figure 1(b). The arrows over the array show the order of chunks and blocks. The blocks and the array cells in each block are serialized in a row-major order.

The size of the chunk is defined by the user, and the size of the block depends on the SEACOW parameter. Suppose  $\mathbb{A}$  is an  $m$  dimensional array. Let  $\mathbb{D}' = \{d'_0, d'_1, \dots, d'_{m-1}\}$  be the chunk dimensions and  $\mathbb{D}'' = \{d''_0, d''_1, \dots, d''_{m-1}\}$  be the block dimensions. Then, it satisfies  $d''_i = d'_i / 2^L$ , where  $L$  is the wavelet transform level of SEACOW which will be described in the next section. Even with the same chunk size, the size of the block decreases as the wavelet transform level increases.

#### 3.3 Wavelet synopsis

The wavelet synopsis of SEACOW summarizes the approximate information about the source array. It is generated as a result of the wavelet transformation. In the wavelet transformation, an array is divided into a set of approximate coefficients and several sets of detail coefficients. The first part containing the approximate

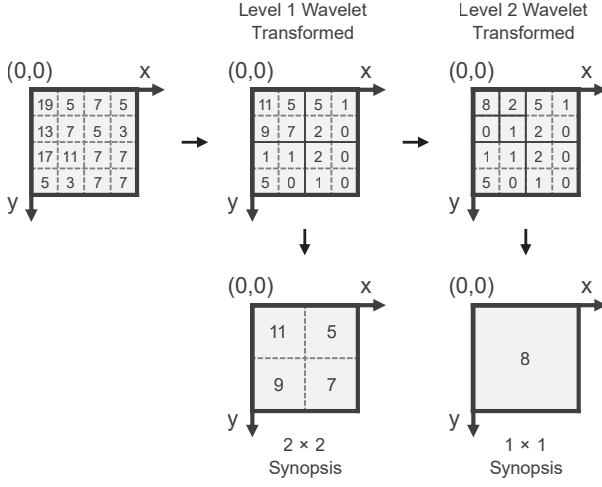


Figure 2: Example of wavelet synopses.

coefficients can be treated as a summary of the original array. We call the approximate coefficients the wavelet synopsis and denote it as  $\mathbb{S}$ .

The wavelet synopsis contents can vary according to the wavelet functions. In our method, SEACOW, we use the Haar wavelet function. In the Haar wavelet transform, the approximate coefficients are obtained by averaging the elements of the neighboring cells. The transformed result is exactly the same as the result of grid aggregation, which splits the array into non-overlapped sub-arrays and applies an average aggregate function to all values of the sub-array.

The wavelet synopsis size could be several times smaller than that of the original array. According to the wavelet transform level  $L$  and the number of dimensions  $||\mathbb{D}||$  of the array. Accordingly, the size of the synopsis is defined as  $||\mathbb{S}|| = \frac{||\mathbb{A}||}{2^{(||\mathbb{D}|| \times L)}}$ , where  $||\mathbb{A}||$  is the size of Array  $\mathbb{A}$ . In this formula,  $||\mathbb{S}||$  can vary in size, even in the same array. It decreases as  $L$  and  $||\mathbb{D}||$  increase. For example, a wavelet synopsis derived from a two-dimensional array with  $L = 4$  has  $\frac{1}{256}$  storage requirement compared to the source array. Furthermore, the one from a three-dimensional array with  $L = 4$  takes only  $\frac{1}{4096}$  storage space.

Figure 2 shows an example of wavelet synopsis using the Haar wavelet transform. In the figure, there are two versions of wavelet synopsis according to  $L$ . The left wavelet synopsis (a) that has  $2 \times 2$  cells is made from the level 1 wavelet-transformed array. On the other hands, the the right one (b) is made from the level 2 wavelet-transformed array. As the second wavelet synopsis has only one cell, and it is the result of aggregating values from the entire array cells. Now, the wavelet synopsis has an average of the array.

### 3.4 HMMT (Hierarchical Min-max Tree)

The HMMT is a tree-like index, hierarchically represents the value ranges of each sub-array. An HMMT was built for each attribute, such as the wavelet synopsis. It is primarily used for array compressions. However, it can also be utilized as an index for value-based exploration query. Figure 3 shows an example of a three-level

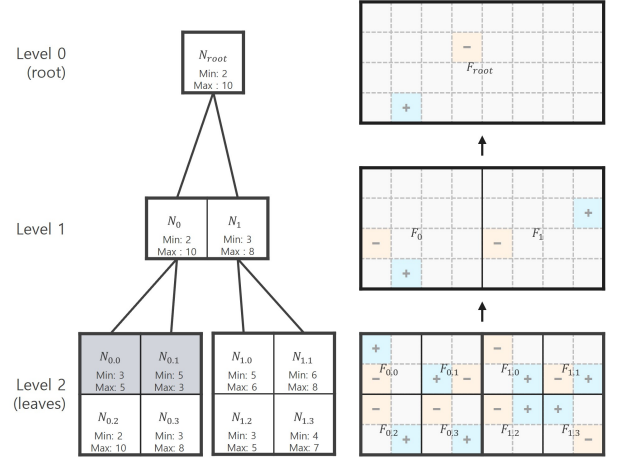


Figure 3: Example of HMMT.

HMMT for a  $4 \times 8$  array. The root node is denoted as  $N_{root}$  and the other ones are denoted as  $N_i$ , where  $i$  denotes its path from the child of the root node, e.g.,  $N_{i,j}$  means the parent node is  $N_i$  and  $j$  is the unique id among the children of  $N_i$ . Except the leaf nodes, each intermediate node  $N_i$  has  $2^{||\mathbb{D}||}$  number of child nodes, where  $||\mathbb{D}||$  is the number of dimensions.

On each tree level, the array is logically partitioned into non-overlapping sub-arrays called fragments. It is not physical partitioning, such as chunks and blocks, and only represents each node's region of interest. The fragment of node  $N_i$  is denoted as  $F_i$  and this relationship is represented as  $F_i \Leftrightarrow N_i$ . In Figure 3,  $F_{root} \Leftrightarrow N_{root}$  and  $F_1 \Leftrightarrow N_1$ . Child fragments are generated by dividing the parent fragment into two on each dimension. For example, in a two-dimensional array, a fragment is split into  $2 \times 2$  child fragments, while, in a three-dimensional array, it is split into  $2 \times 2 \times 2$  child fragments. Yet, The parent fragment includes all the child fragments as follows:

$$F_i = \bigcup \{F_{i,j} \mid j \in \text{CHILD}(i)\}$$

, where the function **CHILD**( $i$ ) returns a set of child node ids of  $N_i$ . For example,  $F_1$  is split into four child fragments:  $F_{1.0}$ ,  $F_{1.1}$ ,  $F_{1.2}$ , and  $F_{1.3}$ . Then, **CHILD**(1) = {0, 1, 2, 3}, while **CHILD**(1.0) =  $\emptyset$  as  $F_{1.0}$  has no child fragment. We also define a function  $\mathcal{R}$  that indicates the smallest fragment  $F_i$  containing all elements of the sub-array  $\mathbb{A}'$  and is denoted as follows:  $\mathcal{R} : \mathbb{A}' \mapsto F_i$ .

Each node  $N_i$  contains two variables  $min$  and  $max$  which are the minimum and maximum elements in the  $F_i$ , respectively.

$$N_i^{\min} = \min(\{x \mid \forall x \in F_i\})$$

$$N_i^{\max} = \max(\{x \mid \forall x \in F_i\})$$

In Figure 3,  $N_{1.3}$  has  $min = 4$  and  $max = 7$ , while its parent node  $N_1$  has  $min = 3$  and  $max = 8$ . As the parent node covers all its child nodes, the relationship of the variables between the child node and the parent node is as follows:

$$N_i^{\min} \leq N_{i,j}^{\min} \leq N_{i,j,k}^{\min}$$

$$N_i^{\max} \geq N_{i,j}^{\max} \geq N_{i,j,k}^{\max}$$

, where  $k \in \text{CHILD}(i, j)$ .

**3.4.1 Building HMMT.** Tree building was performed in a bottom-up fashion. It starts from the leaf nodes. The number of leaf nodes was set as the number of blocks in the array. That is, an HMMT node (also its corresponding fragment) has a one-to-one relationship with a specific block in the array. Accordingly, the leaf level is also called as a *block level* and denoted as  $L_{\text{block}}$ . In  $L_{\text{block}}$ , each node  $N_i$  has the minimum and maximum element in its correlated block  $B_j$ , where  $\mathcal{R} : \mathbb{B}_j \mapsto F_i$  and  $F_i \Leftrightarrow N_i$ . The simple way to find the *min* and *max* of the node is by traversing all elements in the block. After finding *min* and *max* of leaf nodes, the building process moves on to the parent level.

To build the parent level, the child nodes are grouped according to the position of their fragments. Two neighboring child nodes create pairs for each dimension. For the parent node, we do not examine the all value of its fragment to find *min* and *max*. Instead, the variables *min* and *max* of the child nodes are conveyed to the parent node. Then, the parent node takes the minimum and maximum value of them. It is certain that the minimum and maximum element of the fragment can be obtained from the carried values. If the fragment  $F_i$  matches the chunk  $C_i$ , the current tree level is called as *chunk level* and denoted as  $L_{\text{chunk}}$ .

We repeat the step of building parent level until there are not sufficient child nodes to create a group. If merging is no longer available, finally, all nodes in the latest level are grouped to create a  $N_{\text{root}}$ . Then,  $N_{\text{root}}$  has the minimum and maximum elements of the array and  $F_{\text{root}}$  covers the entire array region.

**3.4.2 Encoding HMMT.** The array has several HMMTs according to the number of attributes. The sizes of the HMMTs were not quite large, however, they should be compressed to reduce the overall storage requirement for the array. In each node, there are two variables *min* and *max* to encode. The algorithm exploits the hierarchical relationship of *min* and *max* variables. It employs only differences of the variables between a parent and a child node, not the actual variables. In addition, the differences are converted to a order of significant bit that can guide to an approximation of the variables in decoding process and the tree is substantially compressed. Although, this conversion causes some information loss, the loss does not affect the reconstructing process of the source array.

Algorithm 1 presents the compression process for an HMMT. We assume that the given HMMT is built for an attribute whose data type is  $Ty$ , which requires  $\|Ty\|$  bits. First, let  $\mathcal{B}_n(x)$  be the  $n^{\text{th}}$  significant bits of  $x$  and  $\mathcal{B}(x)$  be the most significant bits (MSB) of  $x$ , in particular. If there is no  $n^{\text{th}}$  significant bits for the value, it returns zero. For example,  $\mathcal{B}(78)$  is 7 as  $78 = (0100\ 1110)_{(2)}$  and  $\mathcal{B}_2(78)$  is 4. In addition, let  $\text{SIGN}(x)$  returns one for  $x \geq 0$  and  $-1$  for  $x < 0$ . Then, we define a  $n^{\text{th}}$  signed significant bits (SSB) as follows:

$$\mathcal{S}_n(x) = \text{SIGN}(x) \times \min(\mathcal{B}_n(|x|), \|Ty\| - 1)$$

, which indicates the sign of  $x$  with  $n^{\text{th}}$  significant bits of its absolute value. For simplicity, we omit  $n$  from  $\mathcal{S}_n(x)$  and denote as  $\mathcal{S}(x)$  when  $n = 1$ . For example, the first signed significant bits of the 78 and  $-78$  are  $\mathcal{S}(78) = 7$  and  $\mathcal{S}(-78) = -7$ .

---

**Algorithm 1:** Encoding algorithm for HMMT

---

**Input** : an HMMT from an array  $A$  with  $\|Ty\|$  bits  
**Output** : a compressed bit-stream of the HMMT

```

1  $N_{\text{root}}^{\text{order}} \leftarrow 1, N_{\text{root}}^{\text{bits}} \leftarrow \text{sizeof}(Ty) \times 8$ 
2  $\mathbb{L}_{\text{node}} \leftarrow \{N_{\text{root}}\}$ 
3  $\text{Comp.flush}()$ 
4 /* Encoding nodes */
5 while  $\mathbb{L}_{\text{node}} \neq \emptyset$  do
6    $N_i \leftarrow \mathbb{L}_{\text{node}}.\text{front}(), n \leftarrow N_i^{\text{order}}, \text{finished} \leftarrow \text{false}$ 
7    $\mathbb{L}_{\text{node}}.\text{pop\_front}()$ 
8    $\mathbb{L}_{\text{child}} \leftarrow \{N_{i,j} \mid j \in \text{CHILD}(i)\}$ 
9   if  $N_i = N_{\text{root}}$  then
10      $\text{Comp.write}(N_i^{\text{min}}, \text{width}=N_i^{\text{bits}})$ 
11      $\text{Comp.write}(N_i^{\text{max}}, \text{width}=N_i^{\text{bits}})$ 
12   else
13      $p \leftarrow \text{PARENT}(i)$ 
14     if  $N_p^{\text{order}} = N_i^{\text{order}}$  then
15        $\text{Comp.write}(\mathcal{S}_n(N_i^{\text{min}}) - \mathcal{S}_n(N_p^{\text{min}}), \text{width}=N_i^{\text{bits}})$ 
16        $\text{Comp.write}(\mathcal{S}_n(N_p^{\text{max}}) - \mathcal{S}_n(N_i^{\text{max}}), \text{width}=N_i^{\text{bits}})$ 
17     else
18        $\text{Comp.write}(\mathcal{S}_n(N_i^{\text{min}}), \text{width}=N_i^{\text{bits}})$ 
19        $\text{Comp.write}(\mathcal{S}_n(N_i^{\text{max}}), \text{width}=N_i^{\text{bits}})$ 
20     end
21   end
22   if  $\mathcal{S}_n(N_i^{\text{min}}) = \mathcal{S}_n(N_i^{\text{max}})$  then
23     /* Hand over next order to the child nodes */
24      $m \leftarrow n + 1$ 
25      $\text{absMax} \leftarrow (\|N_i^{\text{max}}\|)$ 
26     while  $\mathcal{S}_m(N_i^{\text{min}}) = \mathcal{S}_m(N_i^{\text{max}})$  and  $\mathcal{S}_m(N_i^{\text{max}}) \neq 0$  do
27        $m \leftarrow m + 1$ 
28     end
29     if  $\mathcal{S}_m(N_i^{\text{max}}) \neq 0$  then
30        $\text{Comp.write}(m - n, \|\mathcal{S}_n(N_i^{\text{max}})\|)$ 
31     else
32        $\text{Comp.write}(0, \|\mathcal{S}_n(N_i^{\text{max}})\|)$ 
33        $\text{finished} \leftarrow \text{true}$ 
34     end
35      $s \leftarrow \mathcal{S}_n(N_i^{\text{max}}), e \leftarrow \mathcal{S}_m(N_i^{\text{max}})$ 
36      $\text{Comp.write}(\text{absMax}.\text{subtract}(s, e) < 1 \mid 0x1)$ 
37     foreach  $N_{i,j}$  in  $\mathbb{L}_{\text{child}}$  do
38        $N_{i,j}^{\text{order}} \leftarrow m$ 
39        $N_{i,j}^{\text{bits}} \leftarrow \mathcal{S}(\|\mathcal{S}_n(N_i^{\text{max}})\| - 1)$ 
40     end
41   else
42     /* Hand over current order to the child nodes */
43     foreach  $N_{i,j}$  in  $\mathbb{L}_{\text{child}}$  do
44        $N_{i,j}^{\text{order}} \leftarrow N_i^{\text{order}}$ 
45        $N_{i,j}^{\text{bits}} \leftarrow \mathcal{S}(\mathcal{S}_n(N_i^{\text{max}}) - \mathcal{S}_n(N_i^{\text{min}}))$ 
46     end
47   end
48   if not finished then
49      $\mathbb{L}_{\text{node}}.\text{append}(\mathbb{L}_{\text{child}})$ 
50   end
51 end
52 return  $\text{Comp}$ 

```

---

The algorithm is executed in a top-down fashion and starts from the  $N_{root}$ . We temporarily assign two more variables *order* and *bits* in each node, where *order* is a current order of SSB, and *bits* is the number of required bits to encode the node. The *order* and *bits* of the root node are initialized to 1 and  $\|Ty\|$  bits, respectively. Then, we encode the root node (Lines 9-11). The variables *min* and *max* of the root node are encoded in their real values as a starting line.

Then, we set *order* for its child nodes (Line 22-47). It indicates which sequence of SSB should be referred to in the child nodes. The *order* is initialized to one in  $N_{root}$ , starting with the first SSB. However, the *order* can be increased to move on to the next SSB with a specific condition. Suppose the node  $N_i$  is currently being encoded, and  $N_{i,j}$  refers to one of the child node of  $N_i$ , where  $j \in \text{CHILD}(i)$ . Let  $x \in F_i$  and *order* = 1, then,  $x$  satisfies  $N_i^{\min} \leq x \leq N_i^{\max}$ . Accordingly, it also satisfies  $\mathcal{S}(N_i^{\min}) \leq \mathcal{S}(x) \leq \mathcal{S}(N_i^{\max})$ . If  $x$  is varied,  $\mathcal{S}(N_i^{\min})$  and  $\mathcal{S}(N_i^{\max})$  would different. Yet, in case of these two values are equal, all  $x$  in the  $F_i$  have exact the same  $\mathcal{S}(x)$ . This means that it no longer changes in its child nodes. Now, algorithm increases *order* for child nodes and move on to more precise values.

The increase of *order* can be more than one. If the two values are closed to each other, the jumping *order* could be larger. The algorithm finds the next *order* (Line 22-47), then the algorithm writes the difference  $N_{i,j}^{\text{order}} - N_i^{\text{order}}$  (Line 29-34). If there are no further SSB, zero would be encoded. After encoding the jumping *order*, we should also convey the exact value of the mid sector between current *order* and child *order* (Line 35-36). Now,  $N_i$  is encoded, and its child nodes are added in the  $L_{\text{node}}$  to be encoded.

In the child node encoding (Line 12-20), only the delta of  $\mathcal{S}_n(\text{min})$  and  $\mathcal{S}_n(\text{max})$  between the current node and its parent node is encoded. The changes of *min* and *max* variables of a node are only in one direction, continuously decreasing or increasing. Accordingly,  $\mathcal{S}_n(\text{min})$  and  $\mathcal{S}_n(\text{max})$  also have the same trend. If the  $n$  is inherited from the parent node  $N_p^{\text{order}}$ , we encode  $\mathcal{S}_n(N_i^{\min}) - \mathcal{S}_n(N_p^{\min})$  for *min* and  $\mathcal{S}_n(N_p^{\max}) - \mathcal{S}_n(N_i^{\max})$  for *max*, which are always positive or zero. In this representation, we only use  $2 \times \mathcal{S}(\mathcal{S}_n(N_p^{\max}) - \mathcal{S}_n(N_p^{\min}))$  bits. On the contrary, if the  $n$  is advanced in the current node, we newly encode  $\mathcal{S}_n(\text{min})$  and  $\mathcal{S}_n(\text{max})$ . It occupies  $2 \times \mathcal{S}(|\mathcal{S}_n(N_i^{\max})| - 1)$  bits.

### 3.5 Array Compression

The array compression process in SEACOW involves two steps. The first step, a pre-processing step, includes building an HMMT and applying wavelet transform on the source array. The second step, an encoding step, converts the wavelet-transformed array into a compressed bit-stream and writes it in a disk. An overview of the compression process is presented in figure 4.

**3.5.1 Pre-processing.** The pre-processing step for the array compression has three main jobs: (1) building an HMMT from the source array (described in Section 3.4), (2) applying the wavelet transform on the array and (3) redefining the blocks. HMMT provides an estimation of the required bits to encode each part of the array and is important for array compression process. As the HMMT can be

made from the source array, it should be built before the wavelet transform.

When we apply the wavelet transform to the array, the transformation is performed in the chunk unit. We use Haar wavelet in this transformation. During the process, the elements in the chunk are shuffled and the boundary of the block collapses. Therefore, we redraw the block boundaries on each wavelet-transformed chunk. Note that the newly made block looks similar to the previous one, although it has a different region of interest. Suppose that there is an array  $\mathbb{A}$  and its two level wavelet-transformed array  $\mathbb{A}'$ , where the arrays are composed of a single chunk with 16 blocks.  $\mathbb{A}$  and  $\mathbb{A}'$  are shown in Figure 5(a) and (c), respectively. In this figure, the dashed line represents the boundary of block and the solid line represent the boundary of wavelet-transformed sub-arrays. The blocks in Figure 5(a) are mapped to the fragments in Figure 5(b), which have the same size and position of them. However, the blocks in the Figure 5(c) are related to fragments in Figure 5(d), which have different sizes. The relationship depends on the wavelet level of the block belongs. For example,  $B'_7, B'_{13}$ , and  $B'_{15}$  are some of the detail coefficients, where  $L = 1$ . The coefficients are calculated by the elements from  $B_{10}, B_{11}, B_{14}$ , and  $B_{15}$  in Figure 5(a). Furthermore,  $B'_1, B'_4$ , and  $B'_5$  are also detail coefficients, where  $L = 2$ . They are affected by all blocks of  $\mathbb{A}$  from  $B_0$  to  $B_{15}$ . Accordingly,  $\mathcal{R} : \{B'_7, B'_{13}, B'_{15}\} \mapsto F_3$  and  $\mathcal{R} : \{B'_1, B'_4, B'_5\} \mapsto F_{\text{root}}$ .

The blocks of wavelet-transformed chunk are classified as the wavelet synopsis and the body. Each is encoded using different methods. A wavelet transform level  $L$  is a user defining parameter, and it affects the size of wavelet synopsis and compression performance (such as compression ratio, encoding/decoding time, and query execution time). The higher  $L$  can give a higher compression ratio, while, it leads to extended time consumption for encoding and decoding the array. The optimal  $L$  can be obtained experimentally and described in Section 5.1.

**3.5.2 Encoding Array.** In encoding step, we convert the wavelet-transformed array into a compressed bit-stream and write the bit-stream in a disk. As the chunk is the I/O unit, it is independently compressed and decompressed from the disk. The chunks are also split into the blocks. The encoding is performed in order of the blocks in each chunk. The elements of the block  $B_i$  are bit-packed using the minimum number of bits required  $R_i$  to encode without any information loss. It can be found by exploring all elements of  $B_i$  and  $R_i^{\text{real}}$  refer the number from the exploration. It is as follows:

$$R_i^{\text{real}} = \max(\{\mathcal{B}(|x|) \mid \forall x \in B_i\}) + 1$$

where one bit is added to the sign bit at the end of the equation. To convey the exact number of bits used in element encoding, there should be  $B_i$  in a header part of the block. This consumes additional storage space.

Meanwhile, the HMMT can provide an estimate of the required number of bits for a block. Especially, it is certain that all the approximate coefficients of the wavelet synopsis block  $\mathbb{S}_i$  are between  $N_j^{\min}$  and  $N_j^{\max}$ , where  $\mathcal{R} : \mathbb{S}_i \mapsto F_j$  and  $F_j \Leftrightarrow N_j$ . We can assume that the estimate number of the required bits for  $\mathbb{S}_i$  is as follows:

$$R_i^{\text{est}} = \max\left\{\mathcal{B}\left(\left\lceil N_j^{\min} \right\rceil\right), \mathcal{B}\left(\left\lceil N_j^{\max} \right\rceil\right)\right\} + 1$$



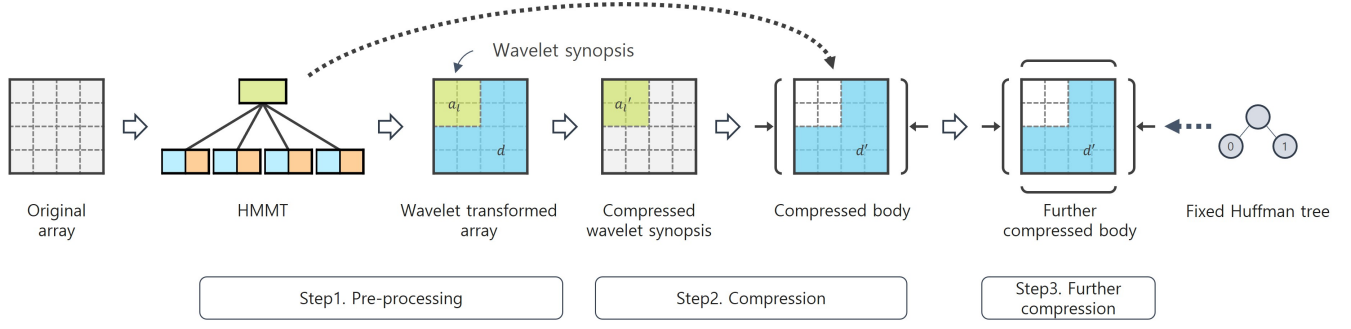


Figure 4: Overview of compression process.

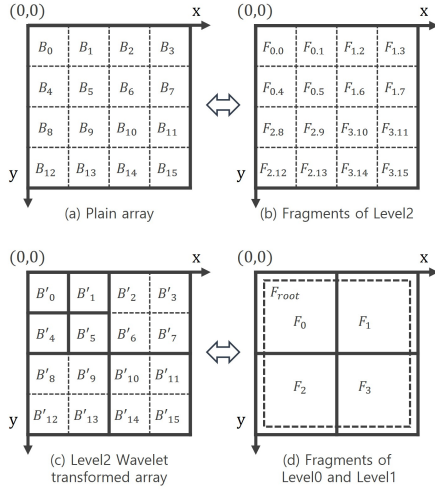


Figure 5: Example of the block in plain array and wavelet-transformed array.

While we can get the exact required number of bits  $R_i^{real}$  from the elements in the block. Then, only the delta  $\Delta_i = R_i^{est} - R_i^{real}$  is recorded in the header of the block, where  $R_i^{est} \leq R_i^{real}$  in the wavelet synopsis block. The all elements are now encoded using  $R_i^{real}$  bits.

The blocks  $B_i$  of the array body part contain detail coefficients, which are the differences between adjacent elements in the Haar wavelet transform. In these type of blocks, we roughly estimate the boundary of these values between  $[N_j^{max} - N_j^{min}, N_j^{max} - N_j^{min}]$ , where  $\mathcal{R} : B_i \mapsto F_j$  and  $F_j \Leftrightarrow N_j$ . Accordingly, the estimate number of the required bit for  $B_i$  is as follows:

$$R_i^{est} = \mathcal{B}(N_i^{max} - N_i^{min}) + 1$$

While, we obtain the  $R_i^{real}$  from the block. Same at the synopsis block, only the delta  $\Delta_i = R_i^{est} - R_i^{real}$  is encoded and the elements are written in the compressed bit-stream using  $R_i^{real}$  bits. In the decoding process, we can easily calculate the  $R_i^{real}$  using  $R_i^{est} - \Delta_i$ , where  $R_i^{est}$  from the HMMT and  $\Delta_i$  from the compressed bit-stream.

In addition, there is an additional option for improving the compression performance. SEACOW uses a fixed-length code to encode the elements in a block. In this fashion, all elements in the same block spent fixed  $R^{real}$  bits. However, it could be inefficient, if there is an outlier that significantly increases  $R^{real}$ . On the other hand, using variable-length coding could be a more capable option. The SEACOW adapts Huffman-coding [8], which is one of the well-known variable-length coding algorithms. It converts a frequently used value (also called symbol) into a short code word, while the less common value is into a long code word. The relationship between the value and code word is written in the Huffman table.

We applied variable-length coding to the body of the compressed array. However, there are several considerations: (1) The blocks of the body part usually have many elements that are close to zero, while they require different  $R_{real}$  bits to encode the their elements. (2) The domain of the elements in the block varies according to  $R^{real}$ . First, we see that the elements in the blocks are generally close to zero, and they look similar to a normal distribution. In the result of the wavelet transform, the significant values are compacted into approximate coefficients. The target blocks for the additional compression contain detailed coefficients, which are less significant values. Our experimental results show that the detail coefficients are more likely to have small values. Secondly, we also see that the blocks have a different distribution of elements depends on the  $R_{real}$  and requires a different Huffman coding table. It is obvious that a block with a high  $R_{real}$  has a wider range of elements, whereas a block with a low  $R_{real}$  has only a narrower range of values. In our datasets, the distributions of elements are not quite different. Therefore, we use several static Huffman coding tables, which are pre-built based on a given frequency distribution. We experimentally obtained the frequency of each element and fitted distribution into a normal distribution function. The function adapts a variation of the distribution  $\sigma^2$  measured experimentally through our data, and the average is fixed as  $\mu = 0$ . Then, we can build the static Huffman coding table only through the probability distribution function.

In the compression process, the blocks are classified by  $R_{real}$  and adapt different static Huffman coding tables. For example, the block contains char data type with 1byte length can have 8 different  $R_{real}$  between  $[0, 8]$ . In this case, there were six different coding tables except for the two exceptional cases where  $R_{real}$  is zero or one.

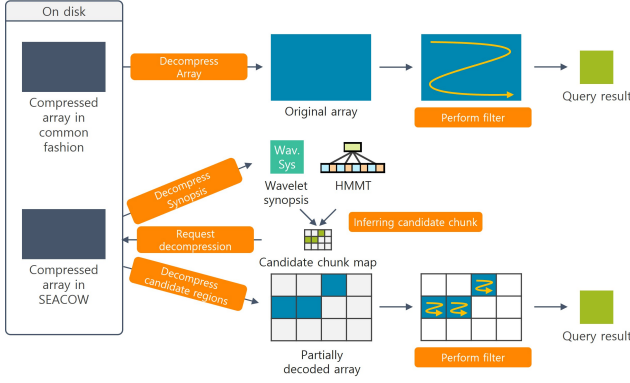


Figure 6: Overview of the filter query processing.

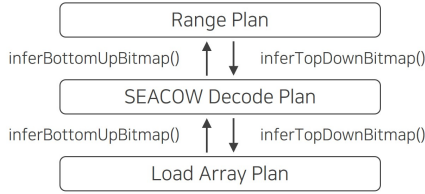


Figure 7: Example of inferring chunk bitmap with a query plan.

## 4 QUERY PROCESSING ON SEACOW

In this section, we present query processing algorithms for SEACOW. In particular, we focus on two types of exploration queries: value-based exploration and dimension-based exploration.

### 4.1 Filter query processing

A value-based exploration query is used to select only the values of interest or find specific data patterns. We use a term filter query to refer to a query that finds a specific element. A simple strategy of filter query can be achieved by loading the entire array from a disk and examining all elements in the array to find the specific element. However, this simple strategy would incur high I/O and computational costs to retrieve and decompress the entire array.

However, if the array has an index for the elements, using an index structure can significantly improve the filter query performance. It is not available in array databases that typically do not hold any value indices. However, SEACOW embeds a synopsis in its compressed bit-stream. Synopsis can be utilized as a value index. More specifically, HMMT helps find a candidate region for the target value of the query. Algorithm 2 shows how to utilize HMMT to find the candidate region.

The algorithm traverses the nodes of the given HMMT  $T$  in breadth-first order. It begins with the root node, which is placed in level zero of  $T$ . The nodes required to iterate is listed in  $N_{cur}$ . The algorithm evaluates each node  $N$  with the given predicate  $p$ , iteratively. The  $N$  has a pair of variables  $min$  and  $max$ , which indicates the range of elements in the matching fragment  $F$ , where  $F \Leftrightarrow N$ . Accordingly, we can estimate whether  $N$  would have elements satisfying  $p$  or not. Suppose that  $p$  specifies to find the value  $v$  in the

---

### Algorithm 2: Finding a candidate region for a filter query using HMMT

---

**Input** : a predicate  $p$  of a filter query, an HMMT  $T$ , a chunk level  $level_{chunk}$ , a block level  $level_{block}$

**Output** : a chunk-block bitmap  $M$

---

```

1  $level \leftarrow 0$ 
2  $N_{cur} \leftarrow \text{GetRootNode}(T)$ 
3 while  $N_{cur} \neq \emptyset$  and  $level \leq level_{block}$  do
4    $N_{next} \leftarrow \emptyset$ 
5   if  $level = level_{chunk}$  then
6     foreach  $N$  in  $N_{cur}$  do
7        $ChunkId \leftarrow \text{GetChunkId}(N)$ 
8       if  $\text{Evaluate}(N, q)$  then
9         /* Set a chunk bitmap */
10         $M[ChunkId] \leftarrow \text{true}$ 
11         $N_{next} \leftarrow N_{next} \cup \text{GetChildNodes}(N)$ 
12      else
13         $M[ChunkId] \leftarrow \text{false}$ 
14      end
15    end
16   else if  $level = level_{block}$  then
17     foreach  $N$  in  $N_{cur}$  do
18        $ChunkId \leftarrow \text{GetChunkId}(N)$ 
19        $BlockId \leftarrow \text{GetBlockId}(N)$ 
20       if  $\text{Evaluate}(N, q)$  then
21         /* Set a block bitmap */
22         $M[ChunkId][BlockId] \leftarrow \text{true}$ 
23       else
24         $M[ChunkId][BlockId] \leftarrow \text{false}$ 
25       end
26     end
27   else
28     foreach  $N$  in  $N_{cur}$  do
29       if  $\text{Evaluate}(N, q)$  then
30         $N_{next} \leftarrow N_{next} \cup \text{GetChildNodes}(N)$ 
31       end
32     end
33   end
34    $level \leftarrow level + 1$ 
35    $N_{cur} \leftarrow N_{next}$ 
36 end

```

---

array. If  $v$  locates outside the range  $[min, max]$ , there should be no element to find. In this case, there is no further action for the child nodes. On the contrary, if the  $v$  is between the  $[min, max]$ , we should further explore its child nodes to get the more specific region of the finding element. Using the fact, a function  $Evaluate$  returns true when  $N$  satisfies the condition of  $p$ , and false otherwise. Meanwhile, there are branches for the two special cases, where the  $level$  is matched the chunk level  $L_{chunk}$  or the block level  $L_{block}$ . At each level, the algorithm finds the chunk and block id for related with  $N$  and marks the corresponding bit of the bitmap  $M$ . As a result of the algorithm, we can get the bitmap that tells the candidate chunks and blocks. The bitmap helps to eliminate unnecessary chunks and blocks for searching and would reduce the computation cost as well as I/O cost.



## 4.2 Range query processing

We use a term range query to refer to a dimension-based exploration query. The range query performance is dependent on the I/O cost of the array. Improving the range query processing performance can be done by excluding the unnecessary chunks outside the query region.

However, general compression schemes are not possible, because they convert an array into a dummy of compressed bit-stream during the compression process. There is no barrier between the blocks, whereas our scheme supports partial decoding in a chunk.

Most importantly, we should know which part of the array to examine for the query in query planning. We should find chunks and blocks that are included or intersected with the query region. The query optimizer examines a query plan tree and inferring a candidate region. The inferring the candidate region on the query plan tree is depicted in figure 7.

Inferring the chunk bitmap involves two steps: (1) Inspection and (2) Propagation. In step (1), the optimizer restricts the query region by referring to the query predicates. This step proceeds from the leaf node to the root node of the query plan tree. Each node of the query tree passes the chunk bitmap to its parent using *inferBottomUpBitmap* function. For a scan query, the optimizer marks all the chunks of the array as it does not know which region of the array will be used for the parent query. On the other hand, for the range query, the optimizer can recognize the exact boundary of the query region according to the given parameters in the query. At the end of step (1), the root has the expected shape of the result array.

However, the I/O job that reads arrays from a disk and uncompresses them is done on the leaf. To reduce the I/O cost, the leaves should recognize the restricted region from step (1). In step (2), the optimizer determines the candidate region of the query from the root to the leaf nodes. Each node of the tree restricts the required chunks and blocks according to the chunk bitmap from its parent node. Then, the node conveys the newly creating chunk bitmap to its child nodes using *inferTopDownBitmap* function.

**Table 2: Detailed specifications of datasets.**

Name	Num cells	Data type	Dimensions	Chunks
Star	1,048,576	uint8	$1,024 \times 1,024$	$16 \times 16$
Saturn	1,048,576	uint8	$1,024 \times 1,024$	$16 \times 16$
Solar	1,048,576	uint8	$1,024 \times 1,024$	$16 \times 16$
Mars	8,388,608	uint8	$4,096 \times 2,048$	$32 \times 16$
Mercury	134,217,728	uint8	$16,384 \times 8,192$	$128 \times 64$
Lunar	3,221,225,472	uint16	$98,304 \times 32,768$	$192 \times 64$

## 5 EXPERIMENTS

In this section, we evaluate the compression ratio and query processing performance of the proposed method. In addition, we compared the query execution time against the existing methods in the following: COMPASS [24], Huffman coding [8], LZW (Lempel-Ziv Welch) [22, 25] and SPIHT [14]. There are also composite compression methods that combine the two existing methods sequentially. LZW+Huffman and SEACOW+Huffman refer to compression

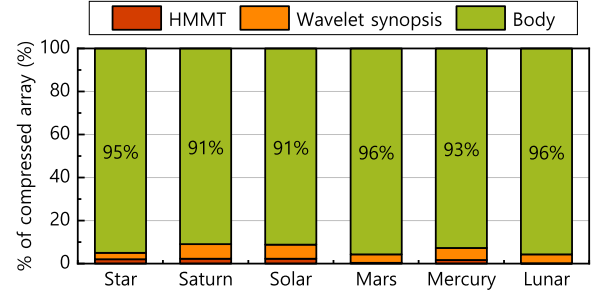


**Figure 8: Percentage of each part of a compressed array. HMMT and wavelet synopsis take up 1.46% and 5.01% of the compressed array on average, respectively. The remaining 93.53% of the compressed array is all occupied by a body of an array.**

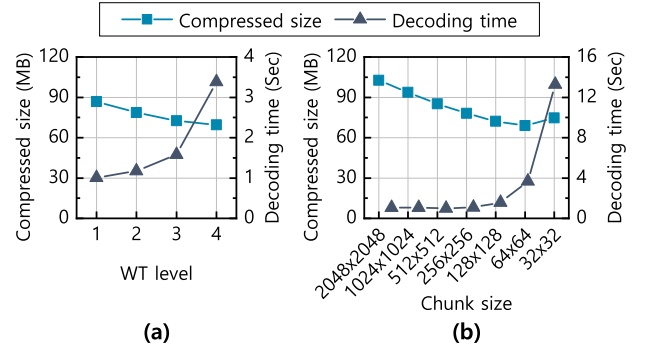


**Figure 9: SEACOW compression performance on Mercury data. (a) the wavelet levels varied from 1 to 4, while the chunk size was fixed as  $128 \times 128$ . (b) the chunk size varied from  $32 \times 32$  to  $2048 \times 2048$ , while the wavelet level was fixed as 3.**

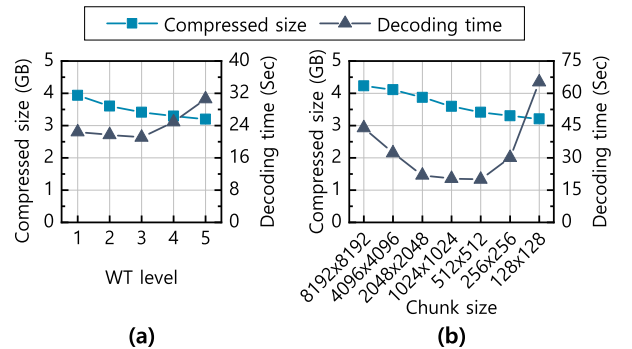


**Figure 10: SEACOW compression performance on Lunar data. (a) the wavelet levels varied from 1 to 5, while the chunk size was fixed as  $512 \times 512$ . (b) the chunk size varied from  $128 \times 128$  to  $8,192 \times 8,192$ , while the wavelet level was fixed as 3.**

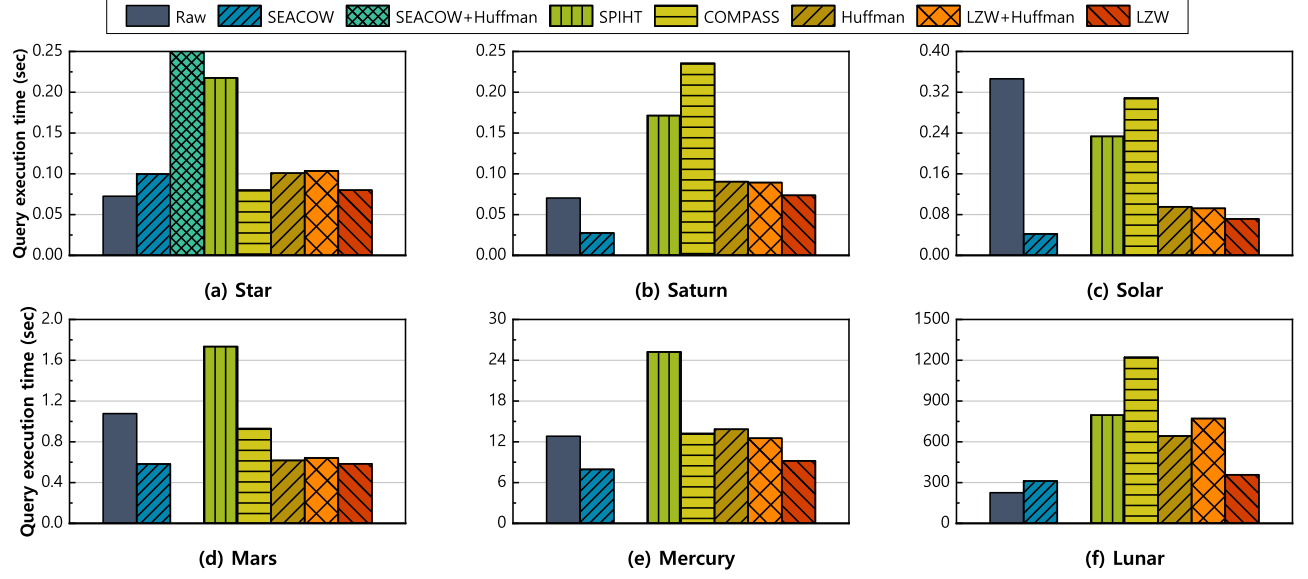


Figure 11: Filter query performance on various datasets.

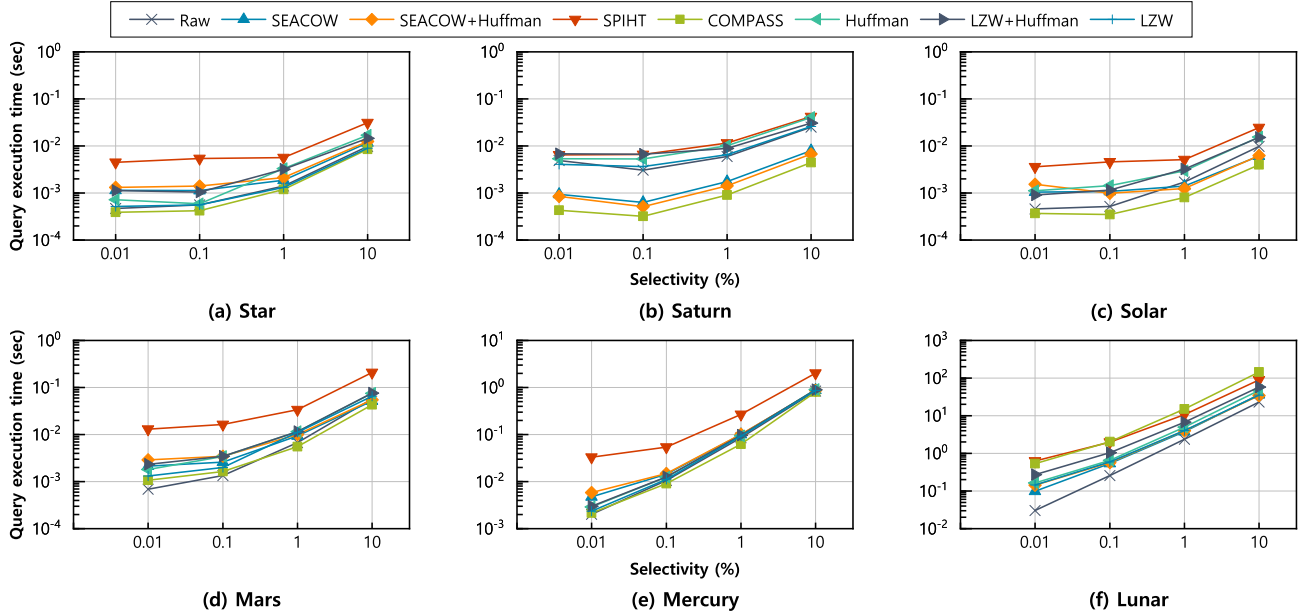


Figure 12: Filter with range selection query performance on various datasets.

schemes that LZW and SEACOW followed by Huffman coding, respectively, and SEACOW+Huffman refer to composite compression schemes that LZW and SEACOW followed by Huffman coding, respectively.

We employed six different real datasets from USGS<sup>1</sup>: Star, Saturn, Solar, Mars, Mercury, and Lunar. They are image data from astronomy. The Star, Saturn, and Solar are small datasets whose

dimension size is  $1,024 \times 1,024$ . These three datasets have all difference features. For example, the Star dataset has sharp contrast with many noise patterns, while the Sun dataset has decent noise patterns. On the other hand, the Saturn dataset is filled with gradation patterns. The Mars, Mercury, and Lunar datasets are planet maps with different resolutions. In particular, Lunar is the largest data that has 2byte numbers, unlike the others. Moreover, Lunar

<sup>1</sup><https://astrogeology.usgs.gov>

**Table 3: HMMT Compression ratio**

Dataset	Raw HMMT	Compressed HMMT	Compression ratio
Star	42.67KB	17.83KB	2.39
Saturn	42.67KB	5.93KB	7.20
Solar	42.67KB	8.90KB	4.79
Mars	85.33KB	25.44KB	3.35
Mercury	1.33MB	0.33MB	4.03
Lunar	8.00MB	1.24MB	6.48

has a largest dimension composed of more than three billion array cells. Table 2 lists the details of the datasets.

We conducted experiments on a Windows machine equipped with an Intel Core i9-11900K (@ 3.50GHz) processor and 64GB of memory, running Windows 10 Enterprise. The datasets were stored in a hard disk with a 2TB 7200rpm SATA. The experiments were performed on our implementation system, called SEACOW storage. It was implemented in C++17. This implementation can be freely accessible at Github<sup>2</sup>.

### 5.1 Compression performance

In this section, we present a compression performance comparison of SEACOW in terms of the chunk size and the wavelet level. We performed comparison on two large datasets (i.e., the Mercury and the Lunar datasets), which are depicted in Figure 9 and Figure 10, respectively. In these figures, the decoding time includes reading a compressed bit-stream from a disk, decompressing the bit-stream, and reorganizing it as a multidimensional array data. First, Figures 9(a) and 10(a) present comparison results on varying wavelet levels, while the chunk size is fixed as  $128 \times 128$  for Mercury data and  $512 \times 512$  for Lunar data. As shown in the results, higher wavelet level makes the compressed array size small, while increases decoding time.

Second, Figures 9(b) and 10(b) present comparison results on varying chunk size, while the wavelet transform level is fixed as 3 in both datasets. In the results, we see that smaller chunk size decreases storage requirements, while it increases the decoding time. Nonetheless, a very tiny chunk size could degrade the compression ratio as it generates many small chunks, all of which have individual metadata that requires additional storage space. Accordingly, use a tiny chunk size would be inefficient for both compression ratio and query performance. As the compression ratio and the query performance have a trade-off, the chunk size and the wavelet level should be balanced considering the compressed size and query performance. Through these experiments, we find efficient parameters for SEACOW compression. In the rest of the experiments, we use 3 wavelet levels and  $64 \times 64$  chunk size.

According to our experiments, SEACOW requires different chunk size and wavelet level depending on the dataset. However, it generates many small fragments and occurs more computational costs for decoding. As a result, the array loading time also increased as the wavelet level goes up.

Table 4 reports the compression ratio on our datasets using 7 different compression schemes. The schemes compress the data

<sup>2</sup><https://github.com/RonyK/SEACOW>

without any information loss. There are also several composite compression methods that combine two existing compression schemes. It is common to combine two or more existing compression schemes in data compression. LZW encoding followed by Huffman coding is LZW+Huffman; likewise, SEACOW encoding followed by Huffman coding is SEACOW+Huffman.

In the table, the composition method of SEACOW+Huffman achieves the highest compression ratio on average. Among the stand-alone methods, SEACOW is the first, and SPIHT is the second. In particular, the following Huffman coding improves the compression performance by 14% on average, with up to 23% in SEACOW. Unlike an array that implicitly represents the position of each array cell, COMPASS should encode the values with its array cell position. Note that Star and Mars have many details. In these datasets, the compression performance of LZW and COMPASS that advance a sequence of similar values were poor.

### 5.2 Value-based exploration performance

This section presents the value-based exploration performance, which is finding specific values in an array. The filter query refers to the value-based exploration. This type of exploration is an essential workflow that is frequently used in data analysis. Figure 11 present the performance of the filter query on various datasets.

Generally, in order to obtain the result of value-based exploration, the entire elements of the array should be evaluated to find the specific value. In the existing compression schemes, the value of each element cannot be determined in a compressed bit-stream. Instead, the compressed array should be decoded to the plain array. SEACOW, on the other hand, has two types of index structures called a synopsis. Utilizing these indexes, SEACOW can select candidate regions where the query results might exist. Subsequently, only the candidate regions are restored to perform the query, which makes the better performance. Similarly, COMPASS also has an index structure. However, the size of its index structure is the same as the compressed array of COMPASS. In order to use the index structure, the whole array should be restored at first. Then, it can fetch the desired values in a specific set of similar elements called a bin.

### 5.3 Dimension-based exploration query performance

This section presents the query performance of a dimension-based exploration with a filter query finding values in a specific region. The range query refers to the dimension-based exploration, and the range-filter query refers to the combination of the dimension and value-based exploration. Since the multidimensional data is large, it is expensive and inefficient to involve the entire array in an analysis query. Instead, it is common that designating the region of interest and performing analysis only in that region. In this experiment, the query performance is affected by the size of the querying region. The selectivity of range querying refers to the percentage of query regions in the entire array space. It is varied from 0.01 to 10. We generated three random regions for each selectivity and reported the average query execution time for these queries.

Figure 12 shows the between-filter query execution time on various datasets. In general, it took more execution time to query

**Table 4: Compression ratio comparison**

Dataset	COMPASS	LZW	Huffman	LZW+Huffman	SPIHT	SEACOW	SEACOW+Huffman
Star	0.92	0.92	1.62	1.20	1.17	1.19	1.49
Saturn	1.38	1.93	2.38	2.27	2.83	3.90	4.45
Solar	1.04	1.37	1.83	1.63	2.19	2.66	3.10
Mars	0.82	0.91	1.33	1.08	1.27	1.26	1.55
Mercury	0.68	1.95	1.19	2.22	1.69	1.83	1.92
Lunar	0.73	1.03	1.13	1.11	1.78	1.76	1.79

on the uncompressed array than the compressed array. SEACOW, on the other hand, shows almost similar performance compared to RAW, and in some cases, narrowly outperformed. In particular, SEACOW is faster than RAW on Saturn and Solar data, which had high compression rates.

The query execution time is increased as the selectivity grows. However, if the query region becomes smaller than the size of the chunk, there would be no significant difference. This is because the chunk is the unit of I/O in SEACOW storage. The small datasets, such as Star, Saturn, and Solar, are partitioned into hundreds of chunks. A range query in this array involves only one or a few adjacent chunks. Thus, in Figure 12(a)-(c), the query execution times are all similar with low selectivity between 0.01% to 1%.

## 6 CONCLUSION

We presented a novel compression algorithm called SEACOW for the multidimensional array. It provides an efficient lossless compression of an array with fast array exploration performance. The proposed method employs a wavelet transform that is widely used in multimedia file compression. Indeed, it shows high compression ratio compared to existing compression algorithms in our experiments. Note that the key difference from the existing methods is that SEACOW embeds an additional data structure called a synopsis, as well as a compressed body of the array. The synopsis is used in the compression process; however, it can also accelerate exploration query processing. Utilizing the feature of synopsis, SEACOW also shows a good performance in the exploration query processing. As a result, the proposed method offers a good trade-off between a compression ratio and an exploration query performance.

There are various applications that can improve performance by utilizing the synopsis, such as calculating an aggregate on each non-overlapped sub-array or finding Top-K values in a specific region. Also, we did not cover progressive query processing on SEACOW. All these subjects can be interesting future work.

## ACKNOWLEDGMENTS

This work was supported by the National Research Foundation of Korea(NRF) grant funded by the Korea government(MSIT) (No. NRF-2020R1A2C2013286).

## REFERENCES

[1] Paul G. Brown. 2010. Overview of sciDB: Large Scale Array Storage, Processing and Analysis. In *Proceedings of the 2010 ACM SIGMOD International Conference on Management of Data* (Indianapolis, Indiana, USA) (SIGMOD '10). ACM, New York, NY, USA, 963–968. <https://doi.org/10.1145/1807167.1807271>

[2] Kaushik Chakrabarti, Minos Garofalakis, Rajeev Rastogi, and Kyuseok Shim. 2001. Approximate query processing using wavelets. *The VLDB Journal* 10, 2 (2001), 199–223.

[3] Dalsu Choi, Chang-Sup Park, and Yon Dohn Chung. 2019. Progressive Top-k Subarray Query Processing in Array Databases. *Proc. VLDB Endow.* 12, 9 (2019), 989–1001. <https://doi.org/10.14778/3329772.3329776>

[4] Philippe Cudré-Mauroux, Hideaki Kimura, K-T Lim, Jennie Rogers, Roman Simakov, Emad Soroush, Pavel Velikhov, Daniel L Wang, Magdalena Balazinska, Jacek Becla, et al. 2009. A demonstration of SciDB: a science-oriented DBMS. *Proceedings of the VLDB Endowment* 2, 2 (2009), 1534–1537. <https://doi.org/10.14778/1687553.1687584>

[5] Manuel Noronha Gamito and Miguel Salles Dias. 2004. Lossless coding of floating point data with JPEG 2000 Part 10. In *Applications of Digital Image Processing XXVII*, Andrew G. Tescher (Ed.), Vol. 5558. International Society for Optics and Photonics, SPIE, 276 – 287. <https://doi.org/10.1117/12.564830>

[6] Minos Garofalakis and Phillip B Gibbons. 2002. Wavelet synopses with error guarantees. In *Proceedings of the 2002 ACM SIGMOD international conference on Management of data*. 476–487.

[7] Goetz Graefe and Leonard D Shapiro. 1990. *Data compression and database performance*. University of Colorado, Boulder, Department of Computer Science.

[8] David A. Huffman. 1952. A Method for the Construction of Minimum-Redundancy Codes. *Proceedings of the IRE* 40, 9 (Sep. 1952), 1098–1101. <https://doi.org/10.1109/JRPROC.1952.273898>

[9] Mehrdad Jahangiri and Cyrus Shahabi. 2008. Plot Query Processing with Wavelets. In *Scientific and Statistical Database Management, 20th International Conference, SSDBM 2008, Hong Kong, China, July 9-11, 2008, Proceedings (Lecture Notes in Computer Science)*, Bertram Ludäscher and Nikos Mamoulis (Eds.), Vol. 5069. Springer, 473–490. [https://doi.org/10.1007/978-3-540-69497-7\\_30](https://doi.org/10.1007/978-3-540-69497-7_30)

[10] Alexander Kalinin, Ugur Cetintemel, and Stan Zdonik. 2015. Searchlight: Enabling Integrated Search and Exploration over Large Multidimensional Data. *Proc. VLDB Endow.* 8, 10 (June 2015), 1094–1105. <https://doi.org/10.14778/2794367.2794378>

[11] M.W. Marcellin, M.J. Gormish, A. Bilgin, and M.P. Boliek. 2000. An overview of JPEG-2000. In *Proceedings DCC 2000. Data Compression Conference*. 523–541. <https://doi.org/10.1109/DCC.2000.838192>

[12] Stavros Papadopoulos, Kushal Datta, Samuel Madden, and Timothy Mattson. 2016. The TileDB Array Data Storage Manager. *Proc. VLDB Endow.* 10, 4 (Nov. 2016), 349–360. <https://doi.org/10.14778/3025111.3025117>

[13] Dimitris Sacharidis, Antonios Deligiannakis, and Timos Sellis. 2009. Hierarchically compressed wavelet synopses. *The VLDB Journal* 18, 1 (2009), 203–231.

[14] A. Said and W.A. Pearlman. 1996. A new, fast, and efficient image codec based on set partitioning in hierarchical trees. *IEEE Transactions on Circuits and Systems for Video Technology* 6, 3 (June 1996), 243–250. <https://doi.org/10.1109/76.499834>

[15] Cyrus Shahabi, Mehrdad Jahangiri, and Farnoush Banaei Kashani. 2008. ProDA: An End-to-End Wavelet-Based OLAP System for Massive Datasets. *Computer* 41, 4 (2008), 69–77. <https://doi.org/10.1109/MC.2008.130>

[16] J.M. Shapiro. 1993. An embedded hierarchical image coder using zerotrees of wavelet coefficients. In *[Proceedings] DCC '93: Data Compression Conference*. 214–223. <https://doi.org/10.1109/DCC.1993.253128>

[17] Emad Soroush, Magdalena Balazinska, and Daniel Wang. 2011. ArrayStore: A Storage Manager for Complex Parallel Array Processing. In *Proceedings of the 2011 ACM SIGMOD International Conference on Management of Data* (Athens, Greece) (SIGMOD '11). ACM, New York, NY, USA, 253–264. <https://doi.org/10.1145/1989323.1989351>

[18] David Taubman, Erik Ordentlich, Marcelo Weinberger, and Gadiel Seroussi. 2002. Embedded block coding in JPEG 2000. *Signal Processing: Image Communication* 17, 1 (2002), 49–72. [https://doi.org/10.1016/S0923-5965\(01\)00028-5](https://doi.org/10.1016/S0923-5965(01)00028-5)

[19] BryanE Usevitch. 2007. JPEG2000 compatible lossless coding of floating-point data. *EURASIP Journal on Image and Video Processing* 2007 (2007), 1–8.

[20] G.K. Wallace. 1992. The JPEG still picture compression standard. *IEEE Transactions on Consumer Electronics* 38, 1 (Feb 1992), xviii–xxiv. <https://doi.org/10.1109/30.125072>

- [21] Yi Wang, Arnab Nandi, and Gagan Agrawal. 2014. SAGA: Array Storage As a DB with Support for Structural Aggregations. In *Proceedings of the 26th International Conference on Scientific and Statistical Database Management (Aalborg, Denmark) (SSDBM '14)*. ACM, New York, NY, USA, Article 9, 12 pages. <https://doi.org/10.1145/2618243.2618270>
- [22] T. Welch. 1984. A Technique for High-Performance Data Compression. *Computer* 17, 06 (jun 1984), 8–19. <https://doi.org/10.1109/MC.1984.1659158>
- [23] Till Westmann, Donald Kossmann, Sven Helmer, and Guido Moerkotte. 2000. The Implementation and Performance of Compressed Databases. *SIGMOD Rec.* 29, 3 (Sept. 2000), 55–67. <https://doi.org/10.1145/362084.362137>
- [24] Haoyuan Xing and Gagan Agrawal. 2018. COMPASS: Compact Array Storage with Value Index. In *Proceedings of the 30th International Conference on Scientific and Statistical Database Management (Bozen-Bolzano, Italy) (SSDBM '18)*. Association for Computing Machinery, New York, NY, USA, Article 7, 12 pages. <https://doi.org/10.1145/3221269.3223033>
- [25] J. Ziv and A. Lempel. 1977. A universal algorithm for sequential data compression. *IEEE Transactions on Information Theory* 23, 3 (May 1977), 337–343. <https://doi.org/10.1109/TIT.1977.1055714>
- [26] M. Zukowski, S. Heman, N. Nes, and P. Boncz. 2006. Super-Scalar RAM-CPU Cache Compression. In *22nd International Conference on Data Engineering (ICDE'06)*. 59–59. <https://doi.org/10.1109/ICDE.2006.150>